Observations of Alfvénic MHD Activity in the H-1 Heliac

B. D. Blackwell [1], D.G. Pretty [1], J.H. Harris [4], J. Howard [1], M.J. Hole [2], D. Oliver [1], A. Nitsche [1], M. Hegland [3], S.T.A. Kumar [1]

1) Plasma Research Laboratory, and
2) Department of Theoretical Physics, Research School of Physical Sciences and Engineering, and
3) Mathematical Sciences Institute, all of the Australian National University, ACT 0200,AUSTRALIA.
4) Oak Ridge National Laboratory, Tn, USA.
Email: boyd.blackwell@anu.edu.au

Abstract: Magnetic configuration scans in the range $1.1 < \iota_0 < 1.5$ in the H-1 flexible heliac have shown a detailed rotational transform dependence of plasma density and fluctuation spectra. Poloidal Mirnov arrays reveal magnetic fluctuations in the range 1-200kHz in plasma produced by RF heating in H, D and He mixtures ranging from highly coherent, often multi-frequency, to broad band. Both positive (stellarator-like) and negative (tokamak-like) shear are examined, including configurations where the sign of the shear reverses. Data mining techniques, SVD, wavelet and Fourier analysis are applied, typically by SVD spatial decomposition of modes on all coils, then a grouping of SVD eigenfunctions, based on spectral similarity, into fluctuation structures. The thousands of structures found are grouped into a small number (~10) of clusters of similar mode structure. Alfvénic scaling in both density and $k_{||}$ are confirmed, although a scale factor ~3 in frequency remains unexplained. The $k_{||}$ dependence provides a precise experimental determination of the position of rational surfaces (if the shear is low). Several features including observation of correlated density fluctuations indicate large amplitudes. The density fluctuations also provide information about the radial location of the modes. Excitation by fast ions is unlikely in H-1, but can not be ruled out, and excitation mechanisms involving fast electrons or steep thermal gradients are being considered. A significant fraction of clearly non-Alfvénic fluctuations indicate that other instabilities are present, such as interchange or ballooning modes, although the amplitude and mode number evidence available is not conclusive. These and other recent observations of Alfvén activity in a low temperature, basically thermal plasma suggests these phenomena may be more widely present--and thus fundamental to toroidal confinement--- than previously thought.

1. Introduction

The H-1[1] heliac (Fig. 3) is a medium sized helical axis stellarator with major radius R=1m, and average minor radius $\langle r \rangle$ ~ 0.15-0.2 m. Its flexible heliac[2] coil set permits access to a wide range of magnetic configurations, achieved by precise control of the ratio k_h of the helical winding current to the ring coil current, providing rotational transform ι in the range $0.9 < \iota_0 < 1.5$ for $B_0 < 1$T. Magnetic fluctuations in the range 1-200kHz are observed when plasma is produced by RF heating (7MHz, 50-100kW) in gas mixtures of hydrogen and helium or deuterium, chosen to optimise plasma production by hydrogen minority heating and to enable spectroscopic diagnostics. Signals range from highly coherent, often multi-frequency in sequence or simultaneously, to approaching broad band ($\delta f/f$ ~ 0.02-0.5). Fig.1 shows an example of coherent modes exhibiting Alfvén scaling with the time varying plasma density ($1/\sqrt{n_e}$). Configuration scans[3] have shown a detailed rotational transform dependence of plasma density (Fig. 2) and fluctuation spectra, the latter being the subject of this paper.

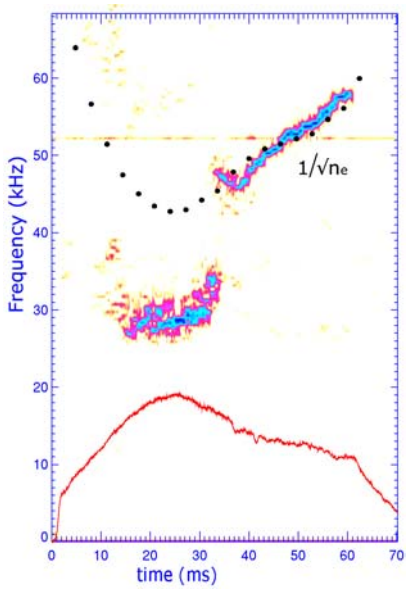

Fig. 1: Evolution of frequency spectra during a discharge for k_h=0.3. Electron density (n_e) is shown for reference, $1/\sqrt{n_e}$ is overlaid (dotted) to illustrate Alfvénic scaling.

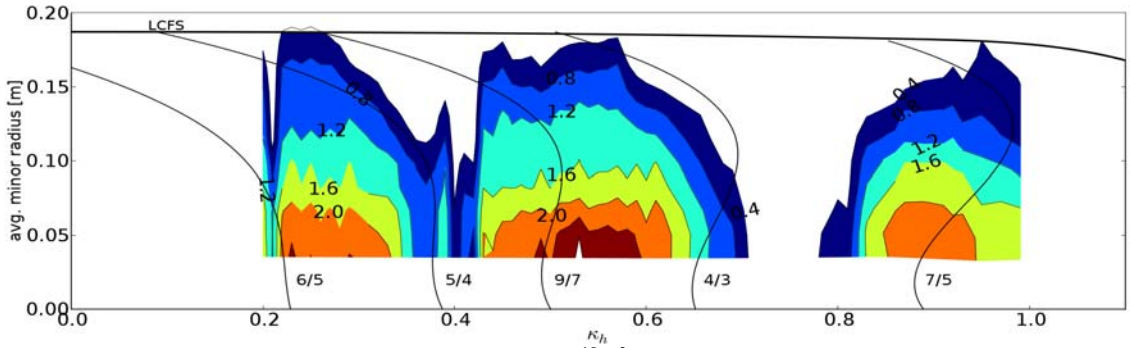

Fig 2. The dependence of electron density profiles($\times 10^{18} m^{-3}$) , important for Alfvén resonance, on configuration ($k_h = I_{Helix}/I_{Ring}$). Lines of constant ι are overlaid, illustrating resonance and shear. Operation is restricted to the range $\kappa_h > 0.16$ and inverted n_e data are not available for $\kappa_h > 1$.

The magnetic probe systems and the data mining process will be described, followed by physical interpretation and relationship to other measurements.

2. Fluctuation Measurements

Poloidal Mirnov arrays of 20 coils (Fig. 4) are located at equivalent positions in two of the 3 toroidal periods (Fig. 3), and there are several other discrete probes. Signals are amplified (1kHz-200kHz, gain ~ 1000x) and digitised. Observations of MHD activity during RF plasma production are presented here for an extensive range of magnetic configurations of both positive (stellarator-like) and negative (tokamak-like) shear, including configurations where the sign of the shear reverses. A complete data set of ~100 configurations is shown in Fig. 5 as frequency spectra, alongside fluctuation data from a 1.5mm microwave scanning density interferometer[4]. The spectra are very similar, showing that the magnetic fluctuations are accompanied by significant density components. Further analysis of the density fluctuation data is presented later. Data mining techniques[5], SVD, wavelet and Fourier analysis are applied in the analysis. The data mining process is largely automated and groups the thousands of structures found into a small number (~10) clusters of similar mode structure. A brief explanation of this data mining process

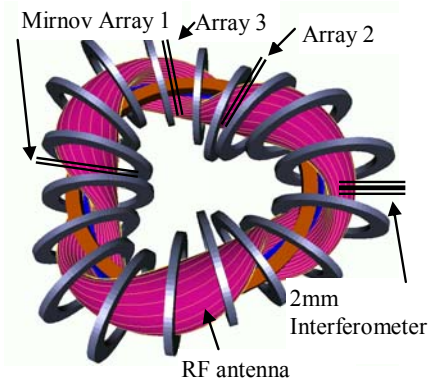

Fig 3: H-1 plasma shown antenna and Mirnov array positions. 18 of 36 TF coils are shown.

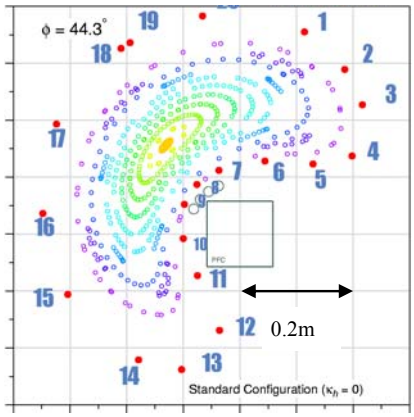

Fig 4: Coil position (numbers) relative to plasma cross-section.

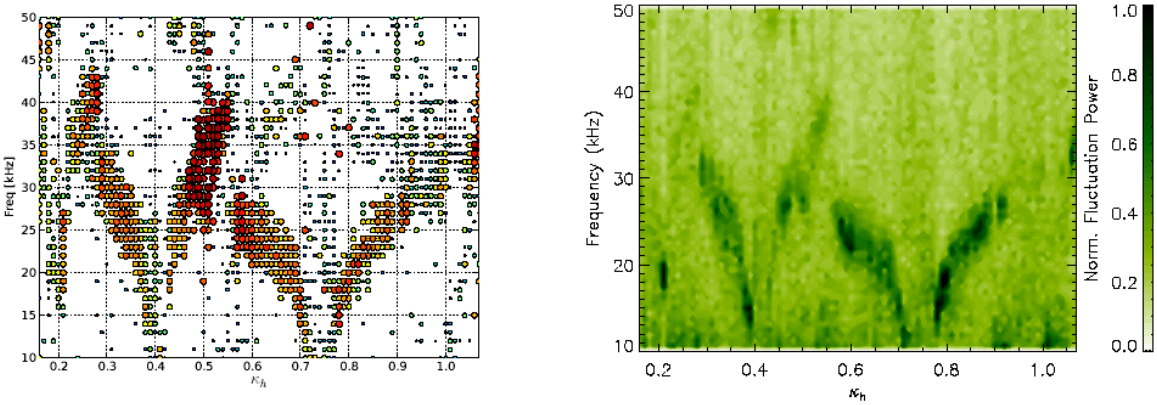

Fig 5: Data from Mirnov coils and swept mm wave interferometer plotted against configuration parameter k_h

is given in the following section.

3. Application of Data Mining

Data mining is the process of extracting useful information from large databases, such as in bio-informatics research where data mining techniques are used to discover useful information in genetic code. In general, the data mining procedure consists of data preprocessing, mining, and interpretation steps. Preprocessing is the stage where existing data are gathered and filtered to maximise the effectiveness of the main data mining algorithm. Here we give an overview of the data mining algorithm used in the analysis of Mirnov signals from H-1, for a more detailed account see[5]. This process is mostly automated and scales well to large datasets.

The data from an arbitrary number of shots can be analysed as a single data set. For each shot, we create an Nc × Ns data matrix Si where Nc is the number of Mirnov channels and Ns is the number of samples. The matrix is split into small time segments to provide time resolution; and for each time segment the singular value decomposition (SVD) is taken. The SVD returns orthogonal pairs of spatial and temporal singular vectors, each with a scalar weighting factor, or singular value SV. From the SVs we can compute the normalised entropy H and normalised energy p of the short time segment [6]. The normalised energy and entropy are used to automatically filter physically interesting signals from noise without any manual investigation of the data itself. To filter the data we require the normalised entropy to be below some threshold H', $0 < H' < 1$, and the normalised energy to be greater than some value p', where $0 < p' < 1$.

We define a *fluctuation structure* as a subset of SVs which have temporal singular vectors with similar power spectra. Each SV is allocated only to a single fluctuation structure and, in general, fluctuation structures will consist of several SVs. To distinguish fluctuation types, we use the set of phase differences between nearest neighbour channels. For each fluctuation structure we take the inverse SVD using its constituent SVs to return to a time series representation for each channel; the set of phase differences between nearest neighbour channels, evaluated at the dominant frequency, is then set as a property of the fluctuation structure.

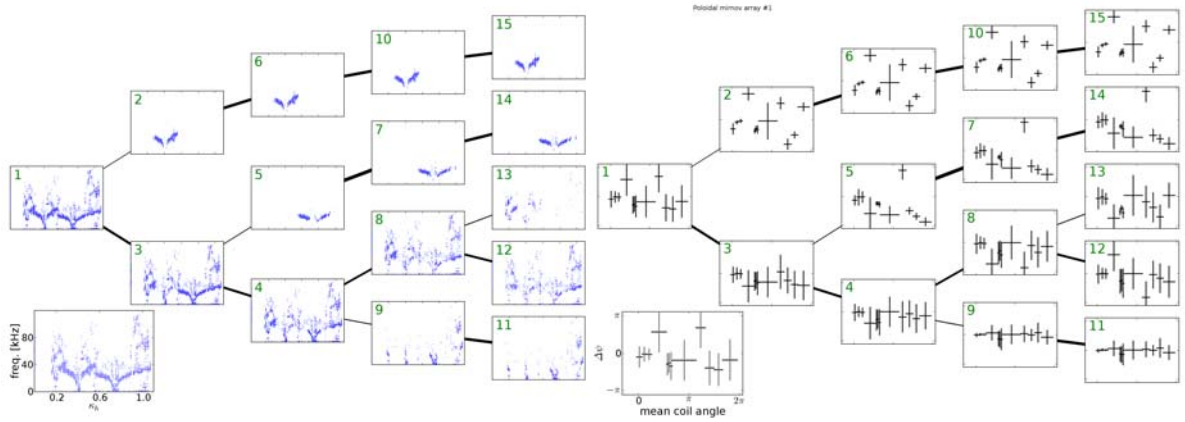

Fig 6 Cluster tree showing (a) clustered data in frequency and configuration space and (b) the cluster definitions in phase space. The first 5 levels are shown here; higher levels show further resolution of fluctuation types, especially for clusters 12 and 13. Clusters 14 and 15 represent the fluctuations around the 4/3 and 5/4 resonant surfaces respectively, while cluster 11 contains (n,m) = (0,0) activity. Only poloidal phase differences for one poloidal Mirnov array are shown in figure (b), which is a projection of the cluster definition in the higher dimensional space of all nearest neighbour coil phases. The vertical error bars are standard deviations of the Gaussians

It is assumed that a class of fluctuations is localised in the Nc-dimensional space of the fluctuation structure phase differences. To locate the classes of fluctuations we use a clustering algorithm, such as the expectation maximisation (EM) algorithm as implemented in the WEKA suite of data mining tools [7]. The identification of the correct number of clusters Ncl, or of which ones are important, is a task that is by no means trivial to automate. We have found a *cluster tree* mapping to be a practical tool for identifying the important clusters, as shown in Fig. 6. The cluster tree displays all clusters for each Ncl below some value, with the clusters for a given Ncl forming a single column. Each cluster is mapped the cluster in Ncl-1 with the largest fraction of common data points. Cluster branches which do not fork over a significant range of Ncl are deemed to be well defined. The point where well defined clusters start to break up again suggests that Ncl is too high.

4. Discussion

Fig. 7 shows the stages of the data mining process. Fig 7a is the result of Fourier decomposition followed by an SVD spatial decomposition of modes on all coils, then a grouping of SVD eigenfunctions, based on spectral similarity, into fluctuation structures. After excluding data below thresholds of entropy (similar to coherence) and normalised energy, and excluding features appearing during plasma formation, clearer structures are visible in Fig 7b. Two "V" shaped features can be seen centred at $k_h \sim 0.4$ and 0.75, the expected position of the $\iota = 5/4$ and 4/3 low order resonances at zero shear, and there is a hint of a third (6/5) near $k_h \sim 0.2$. (operational considerations mean that data are unavailable for $0<k_h<0.16$).

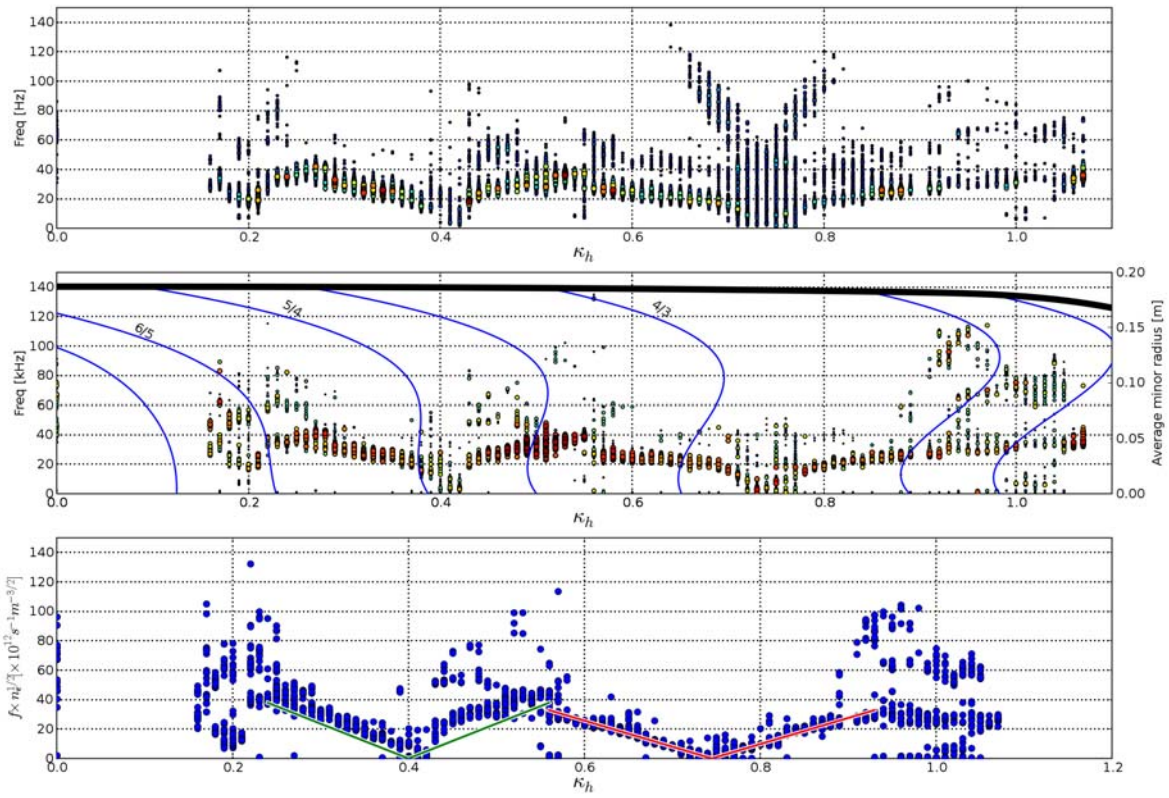

Fig 7. Complete (a) and reduced (b) data sets. Point sizes indicate spectral power density. Entropy and power thresholds have been applied to (b), and each point represents a fluctuation structure reconstructed from SVD eigenfunctions. Loci of rational surfaces are shown. In c) Alfvénic scaling is illustrated (as explained in more detail in relation to figure 4) over the entire data set.

In low shear configurations near (but not at) resonance, global Alfvén eigenmodes (GAEs) [8] are predicted to cluster in the spectral gap $0<\omega<|k_{||}V_A|$ which decreases as the transform approaches resonance (ι = 5/4 and 4/3), and which would lead to minima in f as follows. The Alfvén resonant frequency for the low positive shear typical of H-1 is approximately constant near the axis, and rises steeply toward the plasma edge. Using periodic boundary conditions to close the torus, then $k_{||} = (m/R_0)(\iota - n/m)$, so $\omega \rightarrow 0$ linearly in the vicinity of a resonance (ι = n/m). To search for this dependence in our large dataset, the observed $f^*\sqrt{n_e}$ data from clusters 14 and 15, for a dominant mode is plotted against $k_{||}V_A\sqrt{n_e}$ in fig 8a, and shows good agreement near resonance ($1.29 < \iota < 1.39$). This analysis assumes that the Alfvén instability is radially located at the minimum in Alfvén frequency, taking into account radial profiles of electron density and vacuum rotational transform. When the minimum is zero, the local maximum is chosen, on the assumption that the mode will be localised below this.

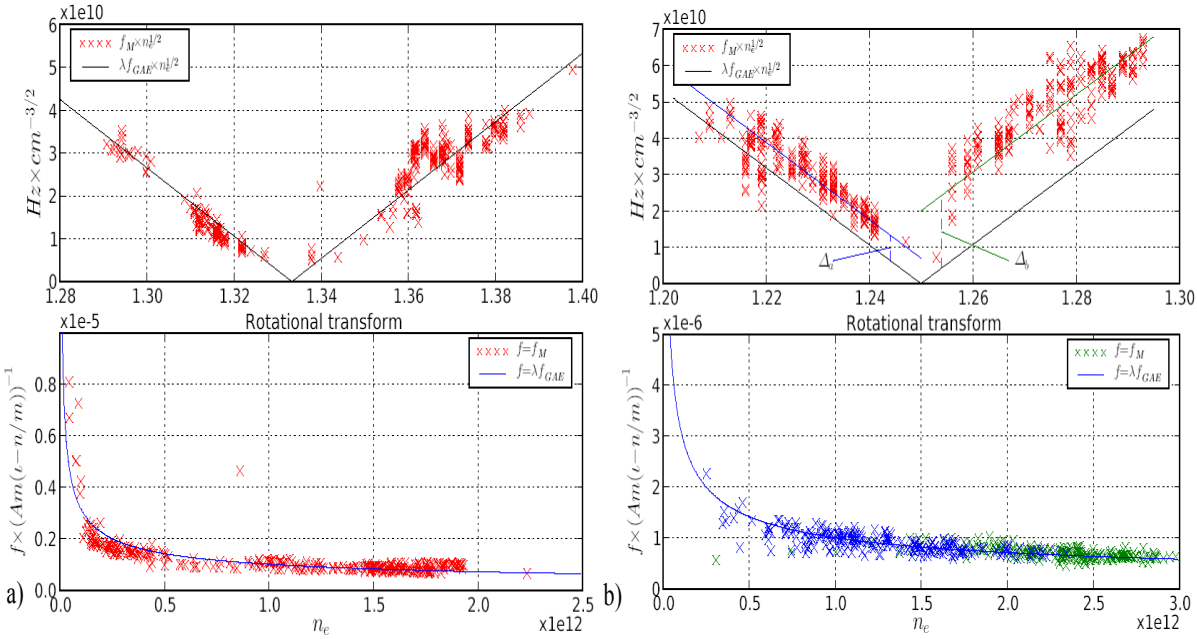

Fig 8: $k_{||}V_A$ (line) compared with observed frequency (kHz, × × ×), both normalized by $\sqrt{n_e}$ for vicinity of the two Y shaped clusters in Fig 7 ($\iota \sim 4/3$ (a) and 5/4 (b)). The lower graphs show the same scaling against n_e rather than ι.

The linear dependence on $\delta\iota$ supports a shear GAE interpretation. A very small offset in transform ($\delta\iota \sim 7\times10^{-3}$) is required for optimal fit to this cylindrical GAE model. This shows that the location of these frequency minima could be an accurate diagnostic of the location of rational iota values. Indeed the correction required is close to the change in ι observed[9] when making electron beam mapping measurements of transform at the unusually high field (for electron beam mapping) of 0.5 Tesla.

Although the dependence in (ι - n/m) is clear, absolute frequency values are lower than predicted by a constant scale factor λ of 1/3. This could be caused by the effective mass density being higher than that of the constituent gas mix due to impurities or momentum transfer to background neutrals, but the extent of both these effects is expected to be too small to explain the entire factor. There is a report[10] of an instability driven by particles travelling at velocity reduced by a comparable scale factor (1/3) and an observation[11] of a toroidal Alfvén eigenmode with spectral components at 1/3 the expected frequency, but the physical mechanism is not clear, and the experimental conditions are somewhat different.

Fig 8b also shows linear dependence on (ι - n/m), but agreement is not as good near $k_h \sim 0.44$, ($1.2 < \iota < 1.3$) in that the spread of points about the fit lines is greater, the fit lines on either side of the resonance have to be offset by slightly different amounts, and they don't intersect at f=0. This might be due to differences in the ι, shear or density profile on either side of the resonance. A similar explanation in terms of linear dependence on (ι - n/m) holds for the Y shaped features in the raw data of figure 7a near 100kHz for $k_h \sim 0.7$. These occur early in time when the density is very low, so the resonant frequency is high. These structures were filtered out in the second datamining step because the errors in the automated determination of electron density were large compared to the low densities.

Density fluctuation profiles (Fig. 9), measured by a fast sweeping interferometer (2ms, 200GHz) are correlated with the magnetic fluctuations and indicate that these modes are large amplitude ($\delta n_e/n_e < 0.05$) and display different frequencies at different radial locations. Two features of the magnetic signals also indicate that the amplitude is large – harmonic structures are often observed, and one mode often gives way to another mode of a different frequency. For example, in Fig. 1, at 33 ms, the mode near 30kHz dies out and in replaced by the mode near 50kHz overlaid with the $1/\sqrt{n_e}$ curve. In Fig 7, in between the "Y" shaped structures identified at the 5/4 and 4/3 resonances, the lower frequency of the two modes seems to dominate at the expense of the higher frequency mode.

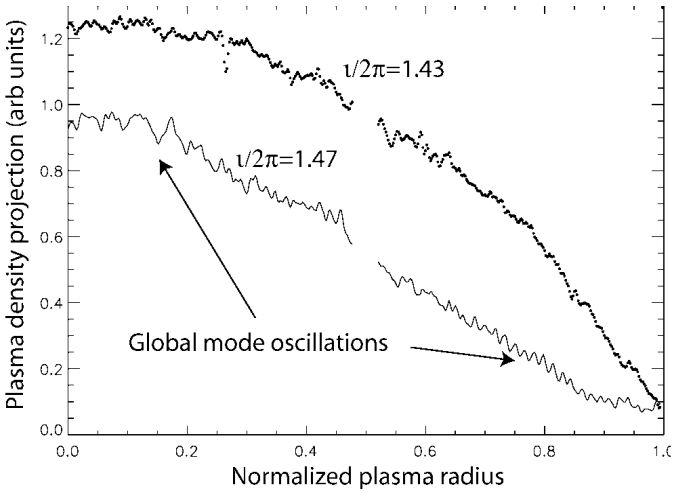

Fig 9: interferometer data showing oscillating and quiescent plasma. The oscillatory time behaviour is aliased into spatial oscillations by the swept interferometer probe beam.

Fast particle driving sources are under investigation, and include both fast electrons and minority-heated H ions. At this time, no clear evidence of suitable fast particles has been found. It is unlikely that H or He ions in H-1 could reach the energy required to match the Alfvén velocity, and there is no obvious spectral indication of high energy components either through charge exchange to H atoms or acceleration of He ions by drag from fast H ions. However both these processes are indirect, and Doppler broadened features due to such high energies would be well into the wings of the spectral lines, and may be difficult to distinguish from the background. There is a distinct possibility of acceleration of either species by the high potential RF (~kV) on the antenna, and it is common to find an elevated temperature in either or both electron and ion species near the edge in RF heated H-1 plasma[12]. Recently observations of excitation of Alfvén eigenmodes by steep temperature gradients, in the absence of high energy tails, have been reported.[13]

Mode structure and possible localisation have been investigated, revealing numbers up to m ~ 6, and including m=3,4, consistent with the explanation of the Alfvén eigenmodes given above. The complex plasma shape (Fig. 4) creates problems in analysis, possibly broadening the poloidal mode spectrum beyond toroidal coupling effects, and variable plasma – probe distance makes mode localisation difficult. Consequently the identification of ballooning modes by observing mode amplitudes in regions of favourable and unfavourable curvature is difficult. However there are clearly some modes which are quite different to the Alfvén eigenmodes described above, either more broadband, or with a density dependence that is

clearly non-Alfvénic. The latter distinction is more obvious when the plasma density varies during a single plasma pulse, and the frequency variation is clearly not $1/\sqrt{n_e}$.

5. Conclusion

Signals from multiple arrays of magnetic probes have been analysed by a datamining procedure which reveals several clusters of phenomena. Some of these clusters are identified as shear Alfvén eigenmodes, most likely GAEs, by identification of both the electron density and $k_{\|}$ dependence. A large amplitude associated density fluctuation has been identified, and features of the magnetic fluctuations corroborate this. Other modes have been found, which may include interchange or ballooning modes, but are awaiting positive identification. Work is in progress to evaluate the effects of the full geometry of H-1 which is far from being cylindrical. The radial resolution of different modes with the electron density interferometer, when coupled with the extensive poloidal and toroidal Mirnov data promises to provide much better resolution of mode structure. The results presented here show that the combination of the flexible, finely controlled H-1 plasma, when coupled with selective ion and electron rf heating, provides a unique controlled environment in which to develop integrated models of Alfvén eigenmodes. Observations of Alfvén activity in a low temperature, basically thermal plasma suggests these phenomena may be more widely present--and thus fundamental to toroidal confinement--- than previously thought, and should enhance the understanding of the impact of Alfvénic activity in modern-day and planned extremely energetic fusion plasmas.

Acknowledgements

The authors would like to thank the H-1 team for continued support of experimental operations as well as R. Dewar, B. McMillan, and T. Luce for useful discussions. This work is supported in part by the U.S. Department of Energy under Contract No. DE-AC05-00OR22725 with UT-Battelle, LLC. This work was performed on the H-1NF National Plasma Fusion Research Facility established by the Australian Government, and operated by the Australian National University, with support from the Australian Research Council Grant DP0344361 and DP0451960.

References

[1] Hamberger S.M., Blackwell B.D., Sharp L.E. and Shenton D.B. "H-1 Design and Construction", *Fusion Technol*. **17**, 1990, p 123.

[2] Harris, J.H., Cantrell, J.L. Hender, T.C., Carreras, B.A. and Morris, R.N. *Nucl. Fusion* **25**, 623 (1985).

[3] Harris J.H., Shats M.G., Blackwell B.D., Solomon W.M., Pretty D.G, et al *Nucl. Fusion,* **44** (2004) 279-286.

[4] Howard J. and Oliver D., "Electronically swept millimetre-wave interferometer for spatially resolved measurement of plasma electron density", accepted for publication, *Applied Optics* (2006)]

[5] Pretty D.G, Blackwell B.D., Harris J.H. "A data mining approach to the analysis of Mirnov coil data from a flexible heliac", submitted to *Plasma Phys. and Contr. Fusion*

[6] Dudok de Wit T, Pecquet A L, Vallet JC, and Lima R. *Phys Plasmas*, **1**(10):3288-3300, 1994

[7] Witten Ian H, and Frank Eibe. Data Mining: *Practical machine learning tools and*

techniques. Morgan Kaufmann, 2nd edition, 2005.

[8] Weller, A., Anton M., et al*., Physics of Plasmas*, 8 (2001) 931-956 and Wong K.L., "A review of Alfvén eigenmode observations in toroidal plasmas" *Plasma Phys. and Contr. Fusion* **41** (1): r1-56 1999

[9] Kumar, S.T.A and Blackwell, B.D, "Modelling the Magnetic Field of the H-1 Heliac", to be submitted to *Rev. Sci. Instruments*.

[10] Biglari H., Zonca F., and Chen L., "On resonant destabilization of toroidal Alfvén eigenmodes by circulating and trapped energetic ions/alpha particles in tokamaks" *Phys. Fluids* B 4 **8** 1992, and
S Ali-Arshad and D J Campbell, "Observation of TAE activity in JET" *Plasma Phys. Control. Fusion* 37 (1995) 715-722.

[11] Maraschek, M., Günter S., Kass T., Scott B., Zohm H., and ASDEX Upgrade Team "Observation of Toroidicity-Induced Alfvén Eigenmodes in Ohmically Heated Plasmas by Drift Wave Excitation", *Phys. Rev. Lett*. **79** 4186-9 1997

[12] Michael C. A., Howard J. and Blackwell B. D., "Measurements and modeling of ion and neutral distribution functions in a partially ionized magnetically confined argon plasma", *Physics of Plasmas* 75, 4180-4182, (2004)].

[13] Nazikian R. et al. *Phys. Rev. Lett*. **96**, 105006 (2006).